UDC 621.375 DOI: 10.18698/0236-3933-2022-1-49-61

COMPARATIVE ANALYSIS OF AEROSOL LIDAR POTENTIAL POSSIBILITIES TO MEASURE WIND SPEED IN DIFFERENT SPECTRAL RANGES

M.L. Belov belov@bmstu.ru
A.A. Samsonova anna.samssonovva@yandex.ru
P.A. Filimonov paulinio91@yandex.ru
S.E. Ivanov ivanov_sergey2@mail.ru
V.A. Gorodnichev gorod@bmstu.ru

Bauman Moscow State Technical University, Moscow, Russian Federation

Abstract

Results are provided of a study devoted to the atmosphere optical state influence on the wind aerosol lidar sensing range and comparison of range estimates obtained for different sensing wavelengths in ultraviolet, visible and near-infrared ranges. It is demonstrated that the aerosol lidar sensing range significantly depends on the Earth atmosphere optical state. The maximum laser sensing range is realized at the wavelength of 1.06 μm dangerous for vision. Sensing wavelengths of 0.355, 1.57 and 2.09 μm are potentially safe for vision. Laser sensing range for the wavelength of 2.09 μm is slightly inferior to the sensing range of 0.355 and 1.57 μm. In this regard, it is promising in the atmosphere surface layer to use sensing wavelengths of 0.355 or 1.57 μm in a wind aerosol lidar. Maximum sensing range of a wind aerosol lidar for a wavelength of 0.355 μm in the transparent earth atmosphere with the receiving lens radius of 150 mm (depending on the laser used) is about 2.5–0.8 km, and for a sensing wavelength of 1.57 μm — about 1.5 km

Keywords

Atmosphere laser sensing, wind speed, aerosol lidar

Received 24.05.2021
Accepted 21.06.2021

Introduction. Laser remote sensing is one of the main methods to monitor the Earth atmosphere parameters. Laser locators (lidars) make it possible to promptly obtain arrays of atmospheric parameters with high temporal and spatial resolution. One of the atmospheric parameters, information about which is used in many practical applications, is the atmosphere wind speed.

Wind speed and direction (in those spatial scales that allow laser sensing) should be known for ensuring the aircraft take-off and landing, eliminating con-

sequences of disasters and emergencies (when harmful or poisonous substances enter the atmosphere), scientific research, environmental protection, etc.

Wind lidars provide remote and prompt acquisition of information about the wind speed and direction based on measuring the aerosol particles motion (under the influence of wind) that are always present in the Earth atmosphere.

Laser methods in measuring wind speed are subdivided into Doppler and correlation methods [1–9]. Despite the fact that aerosol lidars (using the correlation methods) provide a shorter sensing range (compared to the Doppler lidars), they are potentially more attractive in certain practical applications. Such lidars require simpler equipment; they could promptly measure the entire wind speed vector and assess the wind speed spatial distribution along the sensing path without spatial scanning.

One of the most important issues in designing laser systems (including aerosol lidars) is the problem of sensing range.

This work is devoted to comparative analysis of the wind aerosol lidar sensing range, when operating in different spectral ranges (from ultraviolet to near infrared (IR)).

Problem statement. In case of monitoring atmospheric parameters, the sensing wavelength should appear within the atmosphere "transparency windows". Such "transparency windows" are understood as parts of the spectrum with high transmittance (for paths in the atmosphere surface layer, μm: 0.2–0.9; 0.95–1.06; 1.2–1.3; 1.5–1.8; 2.1–2.4; 3.3–4.0; 8–12) [10–13].

Aerosol lidars register radiation scattered by aerosol particles, which largest fractions are ~ 0.1–1.0 μm (submicron fractions). With an increase in the sensing wavelength, radiation fraction scattered "backward" (towards the lidar receiver) is decreasing. Therefore, "transparency windows" are of interest to solve the problem of measuring the wind speed, μm: 0.2–0.9; 0.95–1.06; 1.2–1.3; 1.5–1.8; 2.1–2.4 ("transparency windows" of 3.3–4.0 and 8–12 μm shall not be considered). The atmosphere transmission spectra in ultraviolet, visible and near-IR ranges [13] are presented in Fig. 1.

Comparative analysis of the maximum sensing range for a wind aerosol lidar was carried out in regard to "transparency windows" of 0.2–0.9; 0.95–1.06; 1.2–1.3; 1.5–1.8; 2.1–2.4 μm, and existing laser radiation receivers, and sources (suitable in solving the problem of atmosphere laser sensing with duration of a ns-unit and pulse energy of tens of mJ and more).

Energy of laser radiation scattered by the atmospheric aerosol. Laser correlation methods in atmospheric wind sounding are based on registration of a laser signal scattered by aerosol particles "backward" (towards the lidar). In a general case, energy characteristics calculation of such a signal is a difficult

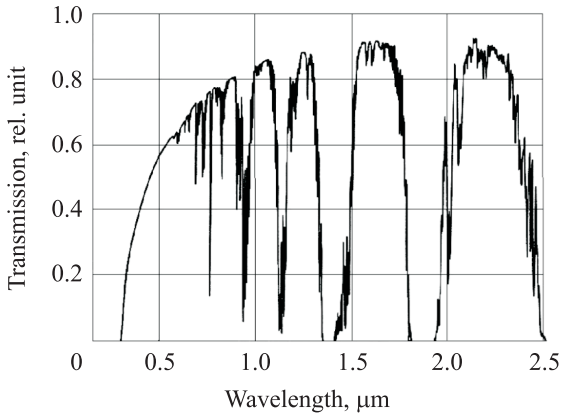

Fig. 1. Atmosphere transmission spectra

task. However, in case of a transparent atmosphere, the $E_s(z)$ expression for energy (or the $P_s(z)$ power) of the received laser signal could be obtained using the single scattering approximation.

It is assumed that the sensing scheme is monostatic. It is believed that at the sensing wavelength in the visible and near-IR spectral regions, optical radiation absorption by atmospheric gases is small (in comparison with attenuation in the aerosol atmosphere). Let us assume that the sensing path is horizontal and moves through the atmosphere surface layer. The monostatic lidar sensing scheme is shown in Fig. 2.

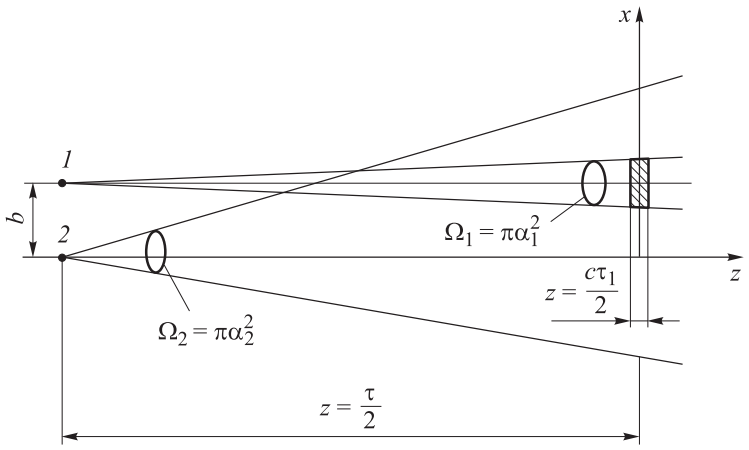

Fig. 2. Monostatic lidar sensing scheme (*1* is emitter; *2* is receiver)

To evaluate the energy of a useful signal (scattered by the atmosphere "backward" towards the lidar) registered by the lidar receiver during detection time in the visible and near-IR spectral regions, let us use the relation (see, for example, [9–12]):

$$E_s(z) = \frac{P_l K_t K_r c \tau_{pulse} r_r^2 \tau_d \sigma \chi_\pi T(z) G(z)}{8z^2}.$$

Here P_l is the lidar radiation power, $P_l = W_{pulse} / \tau_{pulse}$, W_{pulse} is the pulse energy, τ_{pulse} is the lidar pulse duration; K_t, K_r are the transmittance coefficients of the lidar transmitting and receiving optics; c is the speed of light; r_r is the effective radius of the lidar receiving aperture; τ_d is the detection time; χ_π is the Earth atmosphere scattering indicatrix for a scattering angle equal to π (in the "backward" direction to the lidar); σ is the aerosol scattering index; z is the distance to the current atmosphere volume, from which at the $t = 2z/c$ moment of time the signal arrives at the lidar receiver; $T^{1/2}(z) = \exp\left(-\varepsilon z - \kappa_M z\right)$ is the atmospheric transmittance along the lidar — current atmosphere volume path; ε is the atmosphere attenuation index; κ_M is the molecular absorption index (in "transparency windows" of the visible and near-IR regions molecular absorption has insignificant effect); $G(z)$ is the lidar geometric function.

The lidar geometric function has the following form (in the Gaussian approximation) for the sensing scheme shown in Fig. 2 (biaxial monostatic sensing scheme with parallel optical axes of the transmitting and receiving lidar channels):

$$G(z) = \frac{\alpha_r^2}{\alpha_r^2 + \alpha_t^2} \exp\left(-\frac{b^2}{\left(\alpha_r^2 + \alpha_t^2\right) z^2} \right),$$

where α_r, α_t are the field of view of the receiving optical system and the angle of lidar radiation divergence; b is the distance between optical axes of the transmitting and receiving channels (base).

For a monostatic sensing scheme with combined optical axes of the lidar source and receiver, the $G(z)$ function is simplified:

$$G(z) = \frac{\alpha_r^2}{\alpha_r^2 + \alpha_t^2}.$$

Let us use a more general relation (taking into account molecular scattering) in the ultraviolet region of the spectrum to evaluate the $E_s(z)$ energy of a useful signal [10]:

$$E_s(z) = \frac{P_l K_t K_r c \tau_{pulse} r_r^2 \tau_d \left(\sigma \chi_\pi + \sigma_M \chi_{M\pi}\right) \tilde{T}(z) G(z)}{8z^2},$$

where σ_M is the indicator of the atmosphere molecular scattering at the radiation wavelength; $\sigma_M = 0.0119\left(0.55/\lambda\right)^4$, λ are the radiation source wave-

lengths, μm; $\chi_{M\pi}$ is the atmosphere molecular scattering indicatrix for the scattering angle equal to π (in the direction "backward" to the lidar), $\chi_{M\pi} = 0.75\left(1+\cos^2\gamma\right)$, γ is the scattering angle, rad; $\tilde{T}^{1/2}(z) = \exp\left(-\varepsilon z - \sigma_M z - \kappa_M z\right)$ is the atmosphere transmittance along the lidar–current atmosphere volume, taking into account molecular absorption and scattering.

Receiver threshold energy. An estimate of the lidar sensing range could be obtained from the condition of equality of the received lidar signal energy and the minimum detectable (threshold) energy of the lidar receiver.

The $E_{S\min}(\lambda)$ most general expression for the laser signal minimum detectable energy during the τ_d detection time has the following form (for the considered case, i.e., reception of the laser signal scattered by the atmosphere) [10]:

$$E_{S\min}(\lambda) = \frac{1}{2}\mu^2 E(\lambda)\left(1+\left(1+\frac{4}{\mu^2}\left(\frac{E_b(\lambda)}{E(\lambda)}+\frac{i_d+i_j}{2eB^*}\right)\right)^{1/2}\right).$$

Here

$$E(\lambda) = \frac{hcF_G}{\lambda\eta(\lambda)\xi_e};\ B^* = \frac{BF_G}{\xi_e};\ B = \frac{1}{2\tau_d};\ i_j = \frac{2kT}{eG^2\xi_e R_{eq}F_G};$$

$E_b(\lambda)$ is the background radiation energy (during the τ_d detection time); μ is the given signal-to-noise ratio; $\eta(\lambda)$ is the quantum efficiency at the wavelength λ; $e = 1{,}6\cdot 10^{-19}$ A · s is the electron charge; i_d is the dark current (leakage current); i_j is the effective Johnson current; G is the photodetector amplification; F_G is the noise amplification parameter ($F_G \sim 1.0$–2.5); $\xi_e \sim 1$; in calculations it was assumed that $F_G/\xi_e \approx 1$ [10]; R_{eq}, T are the equivalent load resistance of the output circuit and its absolute temperature; h is the Planck's constant; k is the Boltzmann constant.

Background radiation along with the useful laser signal is received by the lidar receiver in ultraviolet, visible and near-infrared ranges due to solar radiation scattered in the Earth atmosphere.

The $E_b(\lambda)$ background radiation energy (during the τ_d detection time) for a lidar with narrow field of view and a narrow-band spectral filter could be represented as (see, for example, [11]):

$$E_b(\lambda) = L_b(\lambda)\Delta\lambda\pi\alpha_r^2 S_r\tau_d,$$

where $L_b(\lambda)$ is the background radiation spectral brightness; $\Delta\lambda$ is the narrow-band filter spectral width; $\pi\alpha_r^2$ is the solid angle of the receiving optical system field of view; $S_r = \pi r_r^2$.

At present, analytical expression for the L_b spectral brightness was obtained only for extremely transparent Earth atmosphere (atmosphere vertical optical depth of $\tau_o \le 0.2$). A specific form of this expression depends on the sensing scheme (sensing in close to horizontal direction, sensing from top to bottom or from bottom to top). Let us assume that sensing is in the atmosphere surface layer in direction close to horizontal. Then for the L_b, we have the following [11]:

$$L_b = 0.25\lambda_s S_\lambda \chi(\gamma) \frac{\cos\theta_o}{\cos\theta - \cos\theta_o}\left(\exp\left(-\frac{\tau_o}{\cos\theta}\right) - \exp\left(-\frac{\tau_o}{\cos\theta_o}\right)\right),$$

where $\lambda_s = \sigma / \varepsilon$; πS_λ is the spectral solar constant at the laser sensing wavelength; $\chi(\gamma)$ is the atmospheric scattering indicatrix; γ is the scattering angle between the solar radiation direction and the direction of the receiver optical axis; θ, φ and θ_o, φ_o are the zenith angles (with respect to the vertical) and the azimuths of the receiver optical axis and the Sun directions, respectively (when calculating, $\varphi = \varphi_o = 0$ was assumed for the sake of clarity); τ_o is the optical depth (in vertical direction) of the entire Earth atmosphere at the sensing wavelength; $\cos\gamma = \cos\theta\cos\theta_o + \sin\theta\sin\theta_o\cos(\varphi - \varphi_o)$.

Study of the atmosphere optical state influence on the sensing range. Let us perform a comparative analysis of potential capabilities (in terms of the sensing range) of an aerosol lidar in different spectral ranges in the atmosphere surface layer.

Most of the time, the Earth atmosphere surface layer stays in a state of haze or foggy haze. Under atmospheric haze, the empirical formula for the $\varepsilon(\lambda)$ attenuation coefficient in the visible and IR spectral ranges has the following form [14]:

$$\varepsilon(\lambda) = \frac{3.91}{S_M}\left(n_o + n_1\lambda^{-n_2}\right), \qquad (1)$$

where S_M is the meteorological visibility range, km; n_o, n_1, n_2 are the empirical coefficients; λ is the radiation wavelength.

Atmospheric haze properties significantly depend both on the year period (winter, summer or spring–autumn) and on the atmosphere optical state at the time of measurement.

Values of the n_o, n_1, n_2 coefficients (obtained experimentally) for different year periods and certain atmosphere optical states are given in [11, 14].

For the aerosol scattering index (see, for example, [11]):

$$\sigma(\lambda) = \frac{\varepsilon(\lambda)}{1 + \alpha(\lambda)}. \qquad (2)$$

Here $\alpha(\lambda)$ is the parameter depending on the wavelength,

$$\alpha(\lambda) = (0.1-0.2)\left(\frac{\lambda}{\lambda_o = 0.55\ \mu\text{m}}\right)^{0.8}.$$

Let us use the empirical formula for the χ_π atmosphere aerosol scattering indicatrix (in the "backward" direction to the lidar):

$$\chi_\pi = 0.33\,\varepsilon(\lambda)^{-0.31}. \quad (3)$$

Along with expression (1), spectral dependence of the haze and foggy haze attenuation index is also approximated by a more coarse, but more convenient formula [10] (in visible and IR spectral ranges):

$$\varepsilon(\lambda) = \frac{3.91}{S_M}\left(\frac{0.55}{\lambda}\right)^{0.585\sqrt[3]{S_M}}. \quad (4)$$

To evaluate the ε aerosol attenuation index in the visible and near-IR spectral ranges (wavelengths of 0.532; 1.06; 1.57 and 2.09 μm), let us use (1)–(4), and for the ultraviolet range — numerical models of the atmosphere optical properties.

For the spectrum ultraviolet range (wavelength of 0.355 μm), let us use the aerosol extinction index value for two atmospheric models. For the continental aerosol optical-location model [15] (this model corresponds to the atmosphere optical state with meteorological visibility range of ~ 15 km), the attenuation index $\varepsilon = 0.337$ km^{-1} (calculation by (4) provides the attenuation index value of 0.489 km^{-1}). For the American model of pure standard atmosphere [16] (this model corresponds to the atmosphere optical state with meteorological visibility range of ~ 25 km), the attenuation index $\varepsilon = 0.24$ km^{-1} (calculation by (4) provides the attenuation index value of 0.329 km^{-1}).

To carry out a comparative analysis of the aerosol lidar potential capabilities for measuring wind speed in different spectral ranges, let us select the following sensing wavelengths, μm: 0.355 (third harmonic of a neodymium-activated YAG laser; in the spectral region lower than 0.355 μm, strong effect of ozone absorption starts); 0.532 (second harmonic of a neodymium-activated YAG laser); 1.06 (fundamental harmonic of a neodymium-activated YAG laser); 1.57 (optical parametric oscillator pumped by a neodymium-activated YAG laser); 2.09 (holmium-activated YAG laser).

When calculating, the sensing path was supposed to be horizontal (atmosphere optical parameters were constant and corresponded to the atmosphere surface layer), the atmosphere was cloudless, and the sensing scheme was monostatic and coaxial. Data from [11] was used for the atmosphere optical depth and for the spectral solar constant at different wavelengths. The μ signal-to-noise

ratio was set equal to 100 (in most cases, the aerosol inhomogeneities contrast is a few percent [9, 17, 18]). The Sun zenith angle was taken equal to $\theta_o = 45°$, the receiving lens radius was 150 mm, the angle of the laser locator radiation divergence was $0.5 \cdot 10^{-3}$ rad, and the receiving optical system field of view was $0.75 \cdot 10^{-3}$ rad. Transmittance of the transmitting and receiving optical systems in calculations were taken equal to 0.9 and 0.7, respectively. Equivalent load resistance and its absolute temperature were equal to $R_{eq} = 10^6$ Ω and $T = 298$ K.

Characteristics of lasers used to calculate the sensing range (pulse energy W_{pulse}, pulse duration τ_{pulse} and repetition rate f_{pulse}) [19–21] for different wavelengths are provided in Tables 1 and 2.

Table 1

Characteristics of various laser models for wavelengths of 0.355 and 0.532 μm

Characteristic	NL319, lamp pumping	NL231-100, diode pumping	LF117, lamp pumping	NL319, lamp pumping	NL231-100, diode pumping	LF117, lamp pumping
$\lambda = 0.355$ μm				$\lambda = 0.532$ μm		
W_{pulse}, mJ	2000	40	150	5000	90	450
τ_{pulse}, ns	4–7	3–7	10–14	4–7	3–7	10–14
f_{pulse}, Hz	10	100	10	10	100	10

Table 2

Characteristics of various laser models for wavelengths of 1.06, 1.57 and 2.09 μm

Characteristic	NL319, lamp pumping	NL231-100, diode pumping	LF117, lamp pumping	CFR400, lamp pumping	HLPN-50-10-40, fiber laser pumping
$\lambda = 1.06$ μm				$\lambda = 1.57$ μm	$\lambda = 2.09$ μm
W_{pulse}, mJ	10 000	150	850	70	50
τ_{pulse}, ns	4–7	3–7	10–14	11	10
f_{pulse}, Hz	10	100	10	10	100

For reception at each wavelength, the following photodetectors were used with the maximum spectral sensitivity [22]: PMT R1924A-100 for 0.355 μm; PMT H8711-300 for 0.532 μm; avalanche photodiode G14858-0020AA for 1.06 μm; avalanche photodiode G8931-20 for 1.57 μm; PIN photodiode G12183-205K for 2.09 μm. Spectral filter width [23]: 2 nm for 0.355 and 0.532 μm; 4 nm for 1.06 μm; 9 nm for 1.57 μm and 80 nm for 2.09 μm.

In the visible and near-IR ranges, calculations were performed for the various atmosphere optical states [11, 14]: 1 is summer period: stable haze, S_M = = 20 km; 2 is summer period: radiation haze, S_M = 15 km; 3 is summer period: radiation haze, S_M = 12 km; 4 is summer period: persistent haze, S_M = 10 km; 5 is winter period: winter haze, S_M = 10 km; 6 is winter period: ice haze, S_M = = 8 km; 7 is winter period: winter haze, S_M = 6 km; 8 is winter period: haze with snow, S_M = 5 km; 9 is spring–autumn period: haze with drizzle, S_M = 3 km; 10 is spring–autumn period: foggy haze, S_M = 2 km.

Calculation results at wavelengths of 0.532 and 1.06 μm for the lamp-pumped lasers are shown in Fig. 3, *a* and *c*. Calculation results for lasers at the wavelength of 0.532 μm with a pulse energy of 5,000 mJ and at the wavelength of 1.06 μm with a pulse energy of 10,000 mJ are not presented, since radiation of these lasers even scattered in the atmosphere is safe only at a distance of more than ~ 400–700 m (GOST 31581–2012. Laser safety. General safety requirements for development and operation of laser products, M., Standartinform, 2013). Calculation results for diode-pumped lasers are shown in Fig. 3, *b* and *d*. Calculation results for wavelengths of 1.57 and 2.09 μm are shown in Fig. 4.

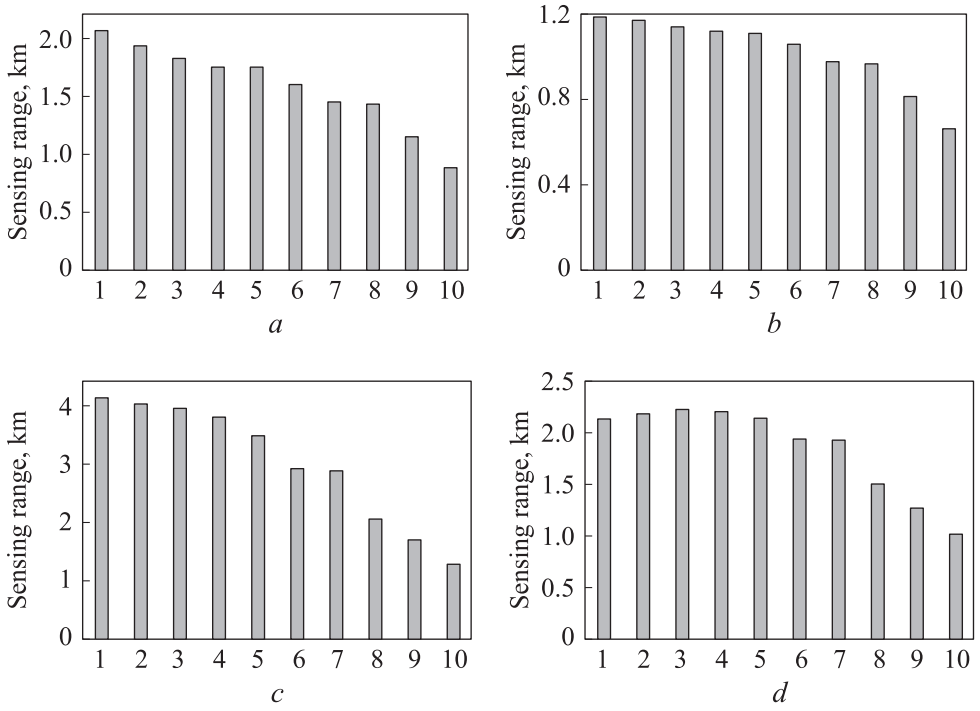

Fig. 3. Sensing ranges at the wavelengths of 0.532 (*a, b*) and 1.06 μm (*c, d*) for lamp-pumped lasers at the pulse energy of 450 (*a*), 850 mJ (*c*) and diode-pumped lasers at the pulse energy of 90 (*b*) and 150 mJ (*d*)

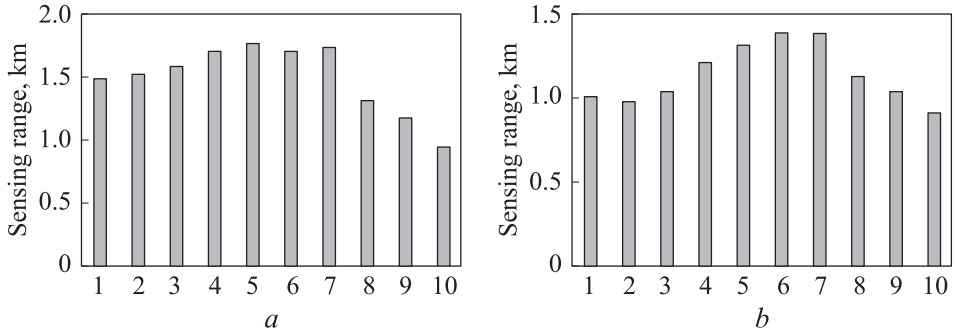

Fig. 4. Sensing ranges at the wavelength of 1.57 (*a*) and 2.09 μm (*b*)

Results of the sensing range evaluation for the wavelength in the ultraviolet spectral region of 0.355 μm are shown in Fig. 5. Here are the results of calculations for two numerical atmosphere models (S_M = 15 and 25 km) for a lamp-pumped laser with the pulse energy of 2,000 mJ (Fig. 5, *a*), lamp-pumped laser with the pulse energy of 150 mJ (Fig. 5, *b*) and diode-pumped laser with the pulse energy of 40 mJ (Fig. 5, *c*). Atmospheric absorption coefficient value for the wavelength of 0.355 μm is taken from [24].

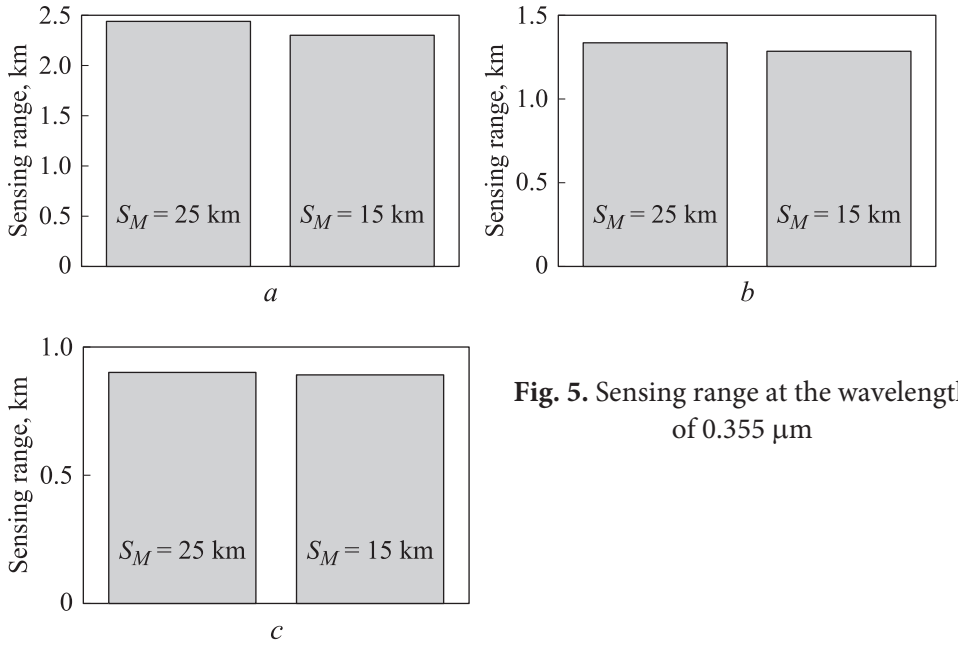

Fig. 5. Sensing range at the wavelength of 0.355 μm

According to the data provided in Fig. 3–5, the aerosol lidar sensing range significantly depends on the atmosphere optical state. For wavelengths of 0.355; 0.532 and 1.06 μm: the smaller is the meteorological visibility range S_M, the shorter is the sensing range. For wavelengths of 1.57 and 2.09 μm, dependence of the sensing range on the S_M meteorological range is more complex.

Naturally, the higher is the energy in a laser pulse, the greater is the sensing range (laser mass and size characteristics will not be discussed in this work). However, spectral dependence of the atmosphere optical characteristics also provides significant influence. The largest sensing range (in the given Figures) is registered in a lamp-pumped laser at the wavelength of 1.06 μm and pulse energy of 850 mJ. For high transparency atmosphere (S_M = 20 km), the sensing range at the wavelength of 1.06 μm and pulse energy of 850 mJ is about 4.2 km, and for cloudy atmosphere (S_M = 2 km) — about 1.3 km.

However, the sensing wavelength of 1.06 μm is hazardous to vision (even radiation scattered in the atmosphere is safe for the eyes only at a distance from the laser beam of more than ~ 110 m for the pulse energy of 850 mJ and ~ 50 m for the pulse energy of 150 mJ).

Wavelengths of 0.355; 1.57 and 2.09 μm are potentially safe for vision. Sensing range for λ = 2.09 μm is somewhat inferior (with the same atmosphere optical conditions) to the sensing range for 0.355 and 1.57 μm. Therefore, it is promising to use sensing wavelengths of 0.355 or 1.57 μm in the atmosphere surface layer with a wind aerosol lidar. For the wavelength of 0.355 μm, radiation scattered in the atmosphere is safe for eyes at the distance from the laser beam more than ~ 7 m for the pulse energy of 2,000 mJ, ~ 2 m for the pulse energy of 150 mJ and ~ 1 m for the pulse energy of 40 mJ. For the wavelength of 1.57 μm, radiation scattered in the atmosphere is safe for the eyes at the distance from the laser beam of more than ~ 0.3 m for the pulse energy of 70 mJ (GOST 31581–2012). In the transparent atmosphere, sensing range for the wavelength of 0.355 μm is (depending on the laser pulse energy) about 2.5–0.8 km, and for the sensing wavelength of 1.57 μm — about 1.5 km.

Conclusion. Influence of the atmosphere optical state on the wind aerosol lidar sensing range was studied, and estimates of the sensing ranges obtained for different wavelengths were compared. It is demonstrated that the lidar sensing range significantly depends on the atmosphere optical state. The maximum sensing range is realized at the wavelength of 1.06 μm, which is dangerous for vision. Potentially safe for vision wavelengths include 0.355; 1.57 and 2.09 μm. Sensing range for 2.09 μm is slightly inferior to the sensing ranges for 0.355 and 1.57 μm. In connection with the above, it appears promising for the atmosphere surface layer to use in a wind aerosol lidar sensing wavelengths of 0.355 or 1.57 μm. In a transparent atmosphere with the receiving lens radius of 150 mm, maximum sensing range for the wavelength of 0.355 μm is (depending on the laser used) approximately 2.5–1.2 km, and for the sensing wavelength of 1.57 μm it is about 1.5 km.

REFERENCES

[1] Banakh V.A., Smalikho I.N., Falits A.V., et al. Stream Line Doppler lidar measurements of wind speed and direction with the duo-beam method in the surface air layer. *Atmos. Ocean. Opt*., 2017, vol. 30, no. 6, pp. 581–587.
DOI: https://doi.org/10.1134/S1024856017060033

[2] Mylapore A.R., Schwemmer G.K., Prasad C.R., et al. A three-beam aerosol backscatter correlation lidar for three-component wind profiling. *Proc. SPIE*, 2014, vol. 9080. DOI: https://doi.org/10.1117/12.2053066

[3] Lane S.E., Barlow J.F., Wood C.R. An assessment of a three-beam Doppler lidar wind profiling method for use in urban areas. *J. Wind Eng. Ind. Aerodyn*., 2013, vol. 119, pp. 53–59. DOI: https://doi.org/10.1016/j.jweia.2013.05.010

[4] Kozintsev V.I., Ivanov S.E., Belov M.L., et al. Laser method of approximate measurement of instantaneous wind velocity and direction. *Optika atmosfery i okeana*, 2013, vol. 26, no. 5, pp. 381–384 (in Russ.).

[5] Wood C.R., Pauscher L., Ward H.C., et al. Wind observations above an urban river using a new lidar technique, scintillometry and anemometry. *Sci. Total Environ*., 2013, vol. 442, pp. 527–533. DOI: https://doi.org/10.1016/j.scitotenv.2012.10.061

[6] Savin A.V., Konyaev M.A. Doppler meteo lidar for systems of ensuring vortex flight safety. *Meteospektr*, 2008, no. 1, pp. 147–152 (in Russ.).

[7] Grishin A.I., Matvienko G.G. Lidar investigations of atmospheric aerosol in the wind shear layers. *Optika atmosfery i okeana*, 1995, vol. 8, no. 7, pp. 1056–1062 (in Russ.).

[8] Matvienko G.G., Samokhvalov I.V., Rybalko V.S., et al. Rate lidar sounding of wind velocity components. *Optika atmosfery i okeana*, 1988, vol. 1, no. 2, pp. 68–72 (in Russ.).

[9] Matvienko G.G., Zade G.O., Ferdinandov E.S., et al. Korrelyatsionnye metody lazerno-lokatsionnykh izmereniy skorosti vetra [Correlation methods of laser-radar measurements of wind speed]. Novosibirsk, Nauka Publ., 1985.

[10] Measures R.M. Laser remote sensing. Fundamentals and applications. Wiley, 1984.

[11] Rozhdestvin V.N., ed. Osnovy impul'snoy lazernoy lokatsii [Fundamentals of impulse laser location]. Moscow, BMSTU Publ., 2010.

[12] Ovcherenko N.E., ed. Optiko-elektronnye sistemy ekologicheskogo monitoringa prirodnoy sredy [Optoelectronic systems of environment ecologic monitoring]. Moscow, BMSTU Publ., 2002.

[13] Jursa A.S., ed. Handbook of geophysics and the space environment. Air Force Geophysics Lab., 1985.

[14] Zuev V.E., ed. Signaly i pomekhi v lazernoy lokatsii [Signals and noises in laser location]. Moscow, Radio i svyaz Publ., 1985.

[15] Krekov G.M., Rakhimov R.F. Optiko-lokatsionnaya model' kontinental'nogo aerozolya [Opto-location model of continental aerosol]. Novosibirsk, Nauka Publ., 1982.

[16] Valley S.B., ed. Handbook of geophysics and space environment. AFCRL, 1965.

[17] Ivanov S.E., Gorodnichev V.A., Belov M.L. Experimentally studied parameters of aerosol inhomogenuities in atmosphere planetary boundary layer at 1.06 μm wavelength. *Proc. SPIE*, 2019, vol. 11208. DOI: https://doi.org/10.1117/12.2540314

[18] Filimonov P.A., Ivanov S.E., Belov M.L., et al. Monitoring of aerosol inhomogeneities parameters in atmosphere at 355 nm. *Proc. SPIE*, 2018, vol. 10833L.
DOI: https://doi.org/10.1117/12.2503652

[19] Nanosecond lasers. *ekspla.com: website*.
Available at: https://ekspla.com/products/nanosecond-lasers (accessed: 02.05.2021).

[20] CFR 400. *ipgphotonics.com: website*.
Available at: https://www.gophotonics.com/products/lasers/quantel-laser/29-168-cfr-400 (accessed: 02.05.2021).

[21] NLPN-50-10-40. *ipgphotonics.com: website*.
Available at: https://www.ipgphotonics.com/en/products/lasers/mid-ir-hybrid-lasers (accessed: 02.05.2021).

[22] Hamamatsu: *company website*.
Available at: https://www.hamamatsu.com/eu/en/index.html (accessed: 02.05.2021).

[23] Semrock: *website*. Available at: http://www.semrock.com (accessed: 02.05.2021).

[24] Belov M.L., Kozintsev V.I., Gorodnichev V.A., et al. Raschet yarkosti fona i oslableniya lazernogo izlucheniya v ul'trafioletovoy oblasti spectra [Calculation of background brightness and laser radiation attenuation in ultraviolet spectral range]. Moscow, BMSTU Publ., 2011.

Belov M.L. — Dr. Sc. (Eng.), Leading Research Fellow, Scientific Research Institute of Radioelectronic and Laser Technology, Bauman Moscow State Technical University (2-ya Baumanskaya ul. 5, str. 1, Moscow, 105005 Russian Federation).

Samsonova A.A. — Master's Student, Department of Laser and Optoelectronic Systems, Bauman Moscow State Technical University (2-ya Baumanskaya ul. 5, str. 1, Moscow, 105005 Russian Federation).

Filimonov P.A. — Engineer, Scientific Research Institute of Radioelectronic and Laser Technology, Bauman Moscow State Technical University (2-ya Baumanskaya ul. 5, str. 1, Moscow, 105005 Russian Federation).

Ivanov S.E. — Cand. Sc. (Eng.), Assoc. Professor, Department of Instrument Elements, Bauman Moscow State Technical University (2-ya Baumanskaya ul. 5, str. 1, Moscow, 105005 Russian Federation).

Gorodnichev V.A. — Dr. Sc. (Eng.), Head of Department of Instrument Elements, Bauman Moscow State Technical University (2-ya Baumanskaya ul. 5, str. 1, Moscow, 105005 Russian Federation).

Please cite this article as:

Belov M.L., Samsonova A.A., Filimonov P.A., et al. Comparative analysis of aerosol lidar potential possibilities to measure wind speed in different spectral ranges. *Herald of the Bauman Moscow State Technical University, Series Instrument Engineering*, 2022, no. 1 (138), pp. 49–61. DOI: https://doi.org/10.18698/0236-3933-2022-1-49-61